Oscillating chiral currents in nanotubes: A route to nanoscale magnetic test tubes

C. J. Lambert and S. W. D. Bailey
Department of Physics, Lancaster University, Lancaster LA1 4YB, United Kingdom

J. Cserti
Department of Physics of Complex Systems, Eötvös University, H-1117 Budapest, Hungary

(Received 31 October 2008; published 15 December 2008)

With a view to optimizing the design of carbon-nanotube (CNT) windmills and to maximizing the internal magnetic field generated by chiral currents, we present analytical results for the group-velocity components of an electron flux through chiral carbon nanotubes. Chiral currents are shown to exhibit a rich behavior and can even change sign and oscillate as the energy of the electrons is increased. We find that the transverse velocity and associated angular momentum of electrons are a maximum for nonmetallic CNTs with a chiral angle of 18°. Such CNTs are therefore the optimal choice for CNT windmills and also generate the largest internal magnetic field for a given longitudinal current. For a longitudinal current of order 10^{-4} A, this field can be of order 10^{-1} T, which is sufficient to produce interesting spintronic effects and a significant contribution to the self-inductance.

DOI: 10.1103/PhysRevB.78.233405 PACS number(s): 73.63.−b, 68.65.−k, 71.15.Ap

Chiral nanotubes and nanowires are of interest for a range of properties associated with external magnetic fields,[1] their potential for creating nanoscale inductors,[2] and their suggested role as building blocks in chiral nanomotors.[3] Examples studied to date include chiral carbon and BC2N nanotubes,[4–6] BN nanotubes,[7] Fe-filled carbon nanotubes (CNTs),[8] and chiral single-wall gold nanotubes.[9]

Most recently, interest in chiral currents has been rekindled by their potential to drive CNT nanometer-scale motors.[10–12] Such motors benefit from low interwall friction[13] and a high tensile strength,[14] which allow one to engineer complex structures,[15–17] including nanoscale bearings,[10,18] rotors,[17,19] oscillators,[20–23] switches,[24] and telescopes.[25] The helical arrangement of the atoms in chiral CNTs can be exploited[26,27] to produce a Brownian ratchet effect,[3] rotational and translational motions driven by thermal gradients,[28,29] and motion[30] induced by circularly polarized light. Recently a drive mechanism for CNT windmills was proposed[31] based on the torque generated by a flux of electrons passing through a chiral CNT. It was shown that under appropriate conditions, the dominant contribution to this torque is proportional to the flux of angular momentum carried by electrons moving in the corresponding infinite chiral CNT. This provides a useful guide for the design of CNT windmills, since a calculation of the angular momentum and associated chiral currents carried by electrons in infinite chiral nanotubes does not require the solution of a scattering problem.

The fact that large chiral currents occur in CNTs is at first sight surprising since early first-principles studies[2,4] suggested that chiral CNTs do not carry a significant chiral current. In this paper we study the energy and voltage dependences of chiral currents in CNTs and show that the small chiral current found in Ref. 4 is a consequence of the metallic nature of the CNT studied. In contrast for nonmetallic CNTs, we predict much larger chiral currents. We find that the energy dependence of chiral currents is surprisingly rich. Indeed the transverse current components can even change sign and oscillate as the energy of the electrons is increased. We demonstrate that the presence of large chiral currents produces significant magnetic fields of order 0.1 T within the volume of a CNT, thereby providing a nanoscale magnetic test tube, which could be used to manipulate the magnetic moments of encapsulated magnetic molecules or particles. This internal field produces a significant contribution to the self-inductance of the CNT, which must be added to the more usual contribution associated with the external magnetic field.[32]

To define the velocity components of electrons in chiral CNTs, we follow the notation of Ref. 33, which introduces the lattice vectors of the corresponding infinite two-dimensional graphene sheet, defined by $\mathbf{a}_1=(\frac{\sqrt{3}}{2},\frac{1}{2})a$ and $\mathbf{a}_2=(\frac{\sqrt{3}}{2},-\frac{1}{2})a$, where $a=\sqrt{3}a_{c\text{-}c}$ and $a_{c\text{-}c}=1.44$ Å is the carbon-carbon bond length. A (n,m) CNT, where $(0\leq m\leq n)$ are integers, is then defined by a transverse chiral vector $\mathbf{Ch}=n\mathbf{a}_1+m\mathbf{a}_2$, which wraps around the CNT circumference and a longitudinal translation vector $\mathbf{T}$. We are interested in resolving electron velocities along axes x and y, which are parallel to the unit vectors $\widehat{\mathbf{Ch}}$ and $\hat{\mathbf{T}}$, respectively. The velocity components are given by $\hbar v_x=\partial E(\mathbf{k})/\partial k_x$ and $\hbar v_y=\partial E(\mathbf{k})/\partial k_y$, where $k_x=\mathbf{k}\cdot\widehat{\mathbf{Ch}}$, $k_y=\mathbf{k}\cdot\hat{\mathbf{T}}$, and $E(\mathbf{k})$ is the energy dispersion relation. In the simplest Slater-Koster scheme, $E(\mathbf{k})$ takes the form[33]

$$E(\mathbf{k})=\gamma\left|1+\exp(-i\mathbf{k}\cdot\mathbf{a}_1)+\exp(-i\mathbf{k}\cdot\mathbf{a}_2)\right|, \qquad (1)$$

where γ is the hopping integral.

Each miniband possesses a continuous longitudinal wave vector k_y and is labeled by a quantized value of k_x given by

$$k_x^q=\frac{2\pi q}{|\mathbf{Ch}|}\quad (q=1,\ldots,N_{\text{hex}}), \qquad (2)$$

where N_{hex} is the number of hexagons in a CNT unit cell. For a given choice of E and q, Eq. (1) can be solved to yield two values of k_y. One of these values, which we denote $k_y^+(q,E)$, corresponds to a positive longitudinal velocity $v_y[q,k_y^+(q,E)]$. The other value, which we denote $k_y^-(q,E)$,

corresponds to a negative longitudinal velocity $v_y[q,k_y^-(q,E)]$. In what follows, we refer to these electrons as "right moving" and "left moving," respectively. We are interested in the transverse velocities of right-moving electrons, which we denote by $v_x[q,k_y^+(q,E)]$. Our aim is to compute the total transverse velocity $v_x^{(n,m)}(E)$ of all right-moving electrons of energy E, which in units of the Fermi velocity v_F is

$$v_x^{(n,m)}(E) = \sum_q v_x[q,k_y^+(q,E)]/v_F, \tag{3}$$

where the sum is over all minibands with real longitudinal wave vectors of energy E.

At low-enough energies, the wave vectors of miniband q (namely, $[k_x^q,k_y^+(q,E)]$ and $[k_x^q,k_y^-(q,E)]$) can be chosen to be close to the K point $\mathbf{K}$. Since $E(\mathbf{k})$ is an even function of $\mathbf{k}$, there will be another pair of wave vectors in the vicinity of the second K point $-\mathbf{K}$, given by $[k_x^{q'},k_y^-(q',E)]=[-k_x^q, -k_y^+(q,E)]$ and $[k_x^{q'},k_y^+(q',E)]=-[k_x^q,k_y^-(q,E)]$, which possesses negative and positive longitudinal group velocities, respectively.

The contribution to the sum in Eq. (3) from these two minibands is

$$\begin{aligned} v_x(q,E) &= v_x[q,k_y^+(q,E)] + v_x[q',k_y^+(q',E)] \\ &= v_x[q,k_y^+(q,E)] + v_x[-q,-k_y^-(q,E)] \\ &= v_x[q,k_y^+(q,E)] - v_x[q,k_y^-(q,E)]. \end{aligned} \tag{4}$$

The last line in this expression is useful because it allows us to focus on the contributions from a single K point only. It also demonstrates that a nonzero transverse velocity arises from trigonal warping since for a perfect Dirac cone, the right-hand side of Eq. (4) would vanish. This suggests that at low energies, an analytical expression for $v_x(q,E)$, can be obtained by writing the electron wave vector in the form $\mathbf{k}=\mathbf{K}+\boldsymbol{\eta}$, where $\mathbf{K}=(0,1)4\pi/(3a)$ is a vector pointing from the origin to a K point and Taylor expanding $E(\mathbf{k})$ as a power series in η_x and η_y, where $\eta_x=\boldsymbol{\eta}\cdot\widehat{\mathbf{Ch}}$ and $\eta_y=\boldsymbol{\eta}\cdot\hat{\mathbf{T}}$. This expansion is of the form

$$E^2 = \sum_{i,j=0}^{\infty} c_{ij}\eta_x^i\eta_y^j, \tag{5}$$

where the coefficients c_{ij} satisfy $c_{00}=c_{10}=c_{01}=c_{11}=0$ and $c_{02}=c_{20}=3\gamma^2/(4a^2)$, $c_{21}=-c_{03}/3=27\gamma^2a^3mn(m+n)/16(n^2+m^2+nm)^{3/2}$, $c_{12}=3\sqrt{3}\gamma^2a^3(m-n)(2n+m)(2m+n)/16(n^2+m^2+nm)^{3/2}$. Differentiating this with respect to η_x and writing $[k_x^q,k_y^{\pm}(q,E)]=\mathbf{K}+(\eta_x,\eta_y^{\pm})$, yields to order $[(\eta_y^{\pm})^2][\eta_x]$,

$$\begin{aligned} 2Ev_x(q,E) = {} & c_{12}[(\eta_y^+)^2-(\eta_y^-)^2] + \eta_x\{2c_{21}[\eta_y^+-\eta_y^-] \\ & + 2c_{22}[(\eta_y^+)^2-(\eta_y^-)^2]\}. \end{aligned} \tag{6}$$

To compute $\eta_y^{\pm}$ for fixed η_x and E, we consider two cases. The first case arises when $\eta_x\neq 0$, in which case one obtains

$$v_x(q,E)/v_F = \frac{2\eta_x c_{21}}{E}\sqrt{E^2/c_{02}-\eta_x^2}. \tag{7}$$

The second case corresponds to $\eta_x=0$. In this case, Eq. (5) yields to lowest order, $E^2=c_{02}\eta_y^2+c_{03}\eta_y^3$, which after solving by iteration and combining with Eq. (6) yields

$$v_x(q,E)/v_F = -c_{03}c_{12}E^2/c_{02}^{5/2}, \tag{8}$$

where $v_F=c_{02}^{1/2}/\hbar=\sqrt{3}\gamma/2a\hbar$ is the Fermi velocity.

Since $k_x=2\pi q/|\mathbf{Ch}|$ and $K_x=\mathbf{K}\cdot\widehat{\mathbf{Ch}}=2\pi(n-m)/3|\mathbf{Ch}|$, the value of η_x for the lowest-energy miniband is $\eta_1=2\pi(-X/3)/|\mathbf{Ch}|$, where $X=1$ for $n=m+1$, $n=m+4$, etc., whereas $X=-1$ for $n=m-1$, $n=m+2$, $n=m+5$, etc. and $X=0$ for $n=m$, $n=m\pm 3$, etc. Values of η_x for higher-energy minibands are obtained from η_1 by adding or subtracting integer multiples of $2\pi/|\mathbf{Ch}|$. For nonmetallic CNTs, where $X=\pm 1$, the value of η_x for the second miniband is $\eta_2=2\pi(2X/3)/|\mathbf{Ch}|$, whereas for metallic CNTs, $\eta_2=\pm 2\pi/|\mathbf{Ch}|$.

For $\eta_j\neq 0$ Eq. (7) yields for the dimensionless transverse velocity associated with channel η_j of a (n,m) CNT

$$v_x^{(n,m)}(\eta_j,E) = v_x(q,E)/v_F = v_j\epsilon_j^{3/2}(\epsilon-\epsilon_j)^{1/2}/\epsilon, \tag{9}$$

where

$$v_j = 3\sqrt{6}mn(n+m)/(n^2+m^2+mn)^{3/2}[\text{sign of } \eta_j]. \tag{10}$$

In this expression, $\epsilon=E/\gamma$ and ϵ_j is the energy minimum of the jth miniband (in units of γ) given by $\epsilon_j=(\sqrt{3}/2)a|\eta_j|$.

The above result applies to all low-energy minibands, except the first miniband of metallic CNTs, for which $\eta_1=0$. In this case, Eq. (8) yields

$$v_x^{(n,m)}(0,E) = \mathrm{v}_0\epsilon^2, \tag{11}$$

where

$$v_0 = \frac{\sqrt{3}mn(m^2-n^2)(2n+m)(2m+n)}{4(n^2+m^2+mn)^3}. \tag{12}$$

This quadratic dependence on ϵ means that low-energy transverse currents in metallic CNTs are indeed small, in agreement with Ref. 4. In contrast the square-root dependence arising when $\eta_j\neq 0$ means that transverse currents in nonmetallic CNTs are predicted to be much larger. This behavior is illustrated in the exact results of Fig. 1, obtained by differentiating Eq. (1) with respect to the transverse and longitudinal wave vectors. For each miniband q the red curves of Fig. 1 show the dimensionless velocities $v_x[q,k_y^+(q,E)]/v_F$ as a function of E for the $(8,m)$ family of CNTs. The black curves show the quantity $v_x^{(n,m)}(E)$, obtained by adding the values of the red curves for each open channel of energy E. As expected, for the achiral (8,8) CNT $v_x^{(n,m)}(E)=0$, whereas for the chiral CNTs $v_x^{(n,m)}(E)\neq 0$.

As well as predicting the energy dependence of transverse velocities, Eqs. (10) and (12) also yield the sign of $v_x^{(n,m)}(\eta_j,E)$. For example, when n and m are positive, the sign of v_1 is equal to the sign of $(-X)$ and therefore for the first open miniband of a (8,4) CNT, $v_x^{(8,4)}(\eta_1,E)$ is negative,

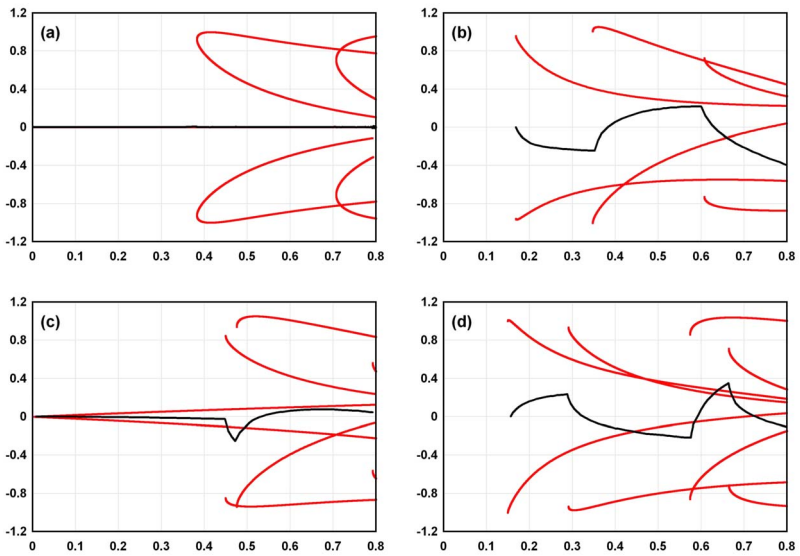

FIG. 1. (Color online) Velocity components for the $(8,m)$ family of CNTs plotted against the energy E (eV), where $m=8,4,5,6$ in (a)–(d), respectively. The red curves show the transverse velocities $v_x[q,k_y^+(q,E)]/v_F$ of right-moving electrons belonging to individual channels q. The black curves show the total velocity $v_x^{(n,m)}(E)$ of Eq. (3).

whereas for the first miniband of a (8,6) CNT, $v_x^{(8,6)}(\eta_1,E)$ is positive. Similarly, when $n\geq 0$ and $m\geq 0$, the sign of v_0 is equal to the sign of $(m\text{-}n)$. Hence, Eq. (12) shows that for the lowest miniband of a (8,5) CNT, $v_x^{(10,4)}(0,E)<0$. For successive higher-energy minibands, η_j alternates in sign and therefore Eqs. (9) and (10) reveal that the transverse velocities of successive higher-energy minibands have a square-root ϵ dependence with an alternating sign. In Eq. (3), the label q sums over $N(E)$ right-moving open channels, where $N(E)$ is a discontinuous function of E, which changes by an integer whenever new channels open or close. As predicted by Eq. (4), the red curves in Fig. 1 show that right-moving channels open or close in pairs and just as a pair of channels open, their tangential velocities cancel. Consequently, as shown in Fig. 1, $v_x^{(n,m)}(E)$ is a continuous function of E, with a discontinuous first derivative.

For the purpose of designing a CNT windmill with the largest torque,[34] or a CNT with the largest internal magnetic field, it is of interest to compute the maximum integrated flux of transverse momentum carried by right-moving electrons in an infinite chiral CNT. Since CNTs with $\eta_1\neq 0$ possess the most favorable energy dependence for $v_x^{(n,m)}(\eta_1,E)$, we focus on nonmetallic CNTs. Since $v_x^{(n,m)}(\eta_1,E)$ and $v_x^{(n,m)}(\eta_2,E)$ have opposite signs, the sum $v_x^{(n,m)}(\epsilon)=v_x^{(n,m)}(\eta_1,E)+v_x^{(n,m)}(\eta_2,E)$ increases monotonically with E for $\epsilon_1\leq\epsilon\leq\epsilon_2$ and then decreases with E for $\epsilon\geq\epsilon_2$, passing through zero when $\epsilon=\epsilon_{\max}$. Hence the maximum integrated flux of transverse velocity is proportional to

$$v_{\max}^{(n,m)}=\int_{\epsilon_1}^{\epsilon_{\max}} d\epsilon v_x^{(n,m)}(\epsilon). \tag{13}$$

From Eq. (9), one obtains $\epsilon_{\max}=15\epsilon_2/14$ and

$$\mathrm{V}_{\max}^{(n,m)}=\frac{\beta mn(n+m)[\text{sign of }(-X)]}{(n^2+m^2+mn)^{5/2}}, \tag{14}$$

where $\beta=2\sqrt{6}\pi^2[4\arctan(\frac{1}{\sqrt{14}})-\arctan(\sqrt{\frac{8}{7}})]\approx 10.9$.

Equation (14) reveals that $v_{\max}^{(n,m)}\to 0$ as $n,m\to\infty$, which reflects the fact that the angular momentum carried by an electron wind is a consequence of the finite diameter of the CNT and the finite difference between successive values of η_j. We also note that the optimum values of (n,m), which maximize $v_{\max}^{(n,m)}$ are those which possess a chiral angle close to $\pi/3-\cos^{-1}\sqrt{11/20}\approx 18°$.

Having analyzed the transverse velocity of electrons in a chiral nanotubes, we now estimate the magnetic field generated by these electrons. In what follows we assume that the chiral CNT can be approximated by a long solenoid with a constant magnetic field B inside the CNT and zero field outside. Since the number of right-moving electrons per unit length in channel q is $(1/\pi\hbar)dE/v_y[q,k_y^+(q,E)]$ and these pass around the circumference of the CNT in a time $\tau=|\mathbf{Ch}|/v_x[q,k_y^+(q,E)]$, the contribution to the tangential current per unit length from the qth miniband is $\{(1/\pi\hbar)dE/v_y[q,k_y^+(q,E)]\}e/\tau$. The magnetic field B inside a solenoid is μ_0 multiplied by the tangential current per unit length. Hence the field due to all right-moving electrons in an energy window eV is

$$B=\frac{2e\mu_0}{h|\mathbf{Ch}|}\int_0^{\mathrm{eV}} dE\sum_q\left\{\frac{v_x[q,k_y^+(q,E)]}{v_y[q,k_y^+(q,E)]}\right\}\Theta\ (E-E_q)], \tag{15}$$

where E_q is the lowest energy of the qth miniband. Since the current carried by these electrons is $I=(1/\pi\hbar)\int_0^{\mathrm{eV}}dE\Sigma_q\Theta[(E-E_q)]$, the magnetic field can be written as $B=\mu_0 I\alpha/|\mathbf{Ch}|$, where

$$\alpha=\frac{\displaystyle\int_0^{\mathrm{eV}} dE\sum_q\left\{\frac{v_x[q,k_x^+(q,E)]}{v_y[q,k_y^+(q,E)]}\right\}\Theta[(E-E_q)]}{\displaystyle\int_0^{\mathrm{eV}} dE\sum_q\Theta[(E-E_q)]}. \tag{16}$$

The dimensionless parameter α is the average ratio of the transverse and longitudinal group velocities. At low voltages, Eq. (4) allows this to be written as a sum over channels near the K point $\mathbf{K}$ and using Eq. (9), one obtains

$$\alpha = \frac{\int_0^{eV} d\epsilon \sum_j \left[\frac{v_j \epsilon_j}{\sqrt{2}} \right] \Theta(\epsilon - \epsilon_j)}{\int_0^{eV} d\epsilon \sum_j \Theta(\epsilon - \epsilon_j)}. \quad (17)$$

For $\epsilon_1 < eV/\gamma < \epsilon_2$, this yields $\alpha = v_1 \epsilon_1 / \sqrt{2}$, which is of order unity for (8,4) or (8,6) CNTs. Consequently, for a current of 10^{-4} A, $|B| \approx 10^{-1}$ T, which is large enough to produce significant spintronic effects,[35] such as rotating the magnetic moment of a small magnetic island[36] or a metallocene encapsulated within a CNT.[37] By computing the energy stored in this magnetic field, we find an associated inductance per unit length of $L = \mu_0 \alpha^2 / 4\pi$. This internal field could be detected through NMR measurements on encapsulated spins and could form the basis of scanning magnetoresistance probe with nanometer spatial resolution. Finally we note that if the longitudinal current is driven by an ac voltage, the oscillations present in $v_x^{(n,m)}(E)$ will lead to the generation of higher harmonics, which may provide an alternative probe of chiral currents.

[1] V. Krstic, G. Wagniere, and G. L. J. A. Rikken, Chem. Phys. Lett. **390**, 25 (2004).
[2] Y. Miyamoto, A. Rubio, S. G. Louie, and M. L. Cohen, Phys. Rev. B **60**, 13885 (1999).
[3] Z. C. Tu and X. Hu, Phys. Rev. B **72**, 033404 (2005).
[4] Y. Miyamoto, S. G. Louie, and M. L. Cohen, Phys. Rev. Lett. **76**, 2121 (1996).
[5] Y. Myamoto, Phys. Rev. B **54**, R11149 (1996).
[6] O. M. Yevtushenko, G. Y. Slepyan, S. A. Maksimenko, A. Lakhtakia, and D. A. Romanov, Phys. Rev. Lett. **79**, 1102 (1997).
[7] P. Král, E. J. Mele, and D. Tomanek, Phys. Rev. Lett. **85**, 1512 (2000).
[8] P. C. P. Watts and W. K. Hsu, Appl. Phys. A: Mater. Sci. Process. **78**, 79 (2004).
[9] R. T. Senger, S. Dag, and S. Ciraci, Phys. Rev. Lett. **93**, 196807 (2004).
[10] J. Cumings and A. Zettl, Science **289**, 602 (2000).
[11] M.-F. Yu, B. I. Yakobson, and R. S. Ruoff, J. Phys. Chem. B **104**, 8764 (2000).
[12] J. W. Kang, K. O. Song, O. K. Kwon, and H. J. Hwang, Nanotechnology **16**, 2670 (2005).
[13] A. N. Kolmogorov and V. H. Crespi, Phys. Rev. Lett. **85**, 4727 (2000).
[14] O. Lourie, D. M. Cox, and H. D. Wagner, Phys. Rev. Lett. **81**, 1638 (1998).
[15] L. Forro, Science **289**, 560 (2000).
[16] P. G. Collins, M. S. Arnold, and Ph. Avouris, Science **292**, 706 (2001).
[17] B. Bourlon, D. C. Glattli, C. Miko, L. Forro, and A. Bachtold, Nano Lett. **4**, 709 (2004).
[18] A. Subramanian, L. X. Dong, J. Tharian, U. Sennhauser, and B. J. Nelson, Nanotechnology **18**, 075703 (2007).
[19] A. M. Fennimore, T. D. Yuzvinsky, W. Q. Han, M. S. Fuhrer, J. Cumings, and A. Zettl, Nature (London) **424**, 408 (2003).
[20] S. B. Legoas, V. R. Coluci, S. F. Braga, P. Z. Coura, S. O. Dantas, and D. S. Galvão, Phys. Rev. Lett. **90**, 055504 (2003).
[21] Q. Zheng and Q. Jiang, Phys. Rev. Lett. **88**, 045503 (2002).
[22] P. A. Williams, S. J. Papadakis, A. M. Patel, M. R. Falvo, S. Washburn, and R. Superfine, Phys. Rev. Lett. **89**, 255502 (2002).
[23] Y. Zhao, C. C. Ma, G. H. Chen, and Q. Jiang, Phys. Rev. Lett. **91**, 175504 (2003).
[24] V. V. Deshpande, H. Y. Chiu, H. W. Ch. Postma, C. Mikó, L. Forró, and M. Brockrath, Nano Lett. **6**, 1092 (2006).
[25] I. M. Grace, S. W. Bailey, and C. J. Lambert, Phys. Rev. B **70**, 153405 (2004).
[26] R. Saito, R. Matsuo, T. Kimura, G. Dresselhaus, and M. S. Dresselhaus, Chem. Phys. Lett. **348**, 187 (2001).
[27] Yu. E. Lozovik, A. V. Minogin, and A. M. Popov, Phys. Lett. A **313**, 112 (2003).
[28] P. A. E. Schoen, J. H. Walther, S. Arcidiacono, D. Poulikakos, and P. Koumoutsakos, Nano Lett. **6**, 1910 (2006).
[29] A. Barreiro, R. Rurali, E. R. Hérnandez, J. Moser, T. Pichler, L. Forró, and A. Bachtold, Science **320**, 775 (2008).
[30] P. Král and H. R. Sadeghpour, Phys. Rev. B **65**, 161401 (2002).
[31] S. W. D. Bailey, I. Amanatidis, and C. J. Lambert, Phys. Rev. Lett. **100**, 256802 (2008).
[32] K. Tsubaki, Y. Nakajima, T. Hanajiri, and H. Yamaguchi, J. Phys.: Conf. Ser. **38**, 49 (2006).
[33] R. Saito, G. Dresselhaus, and M. S. Dresselhaus, *Physical Properties of Carbon Nanotubes* (Imperial College, London, 1998).
[34] A. Kis, K. Jensen, S. Aloni, W. Mickelson, and A. Zettl, Phys. Rev. Lett. **97**, 025501 (2006).
[35] The corresponding magnetic flux $\phi = B|\mathbf{Ch}|^2/(4\pi)$ is given by $\phi/\phi_0 = 1.44\sqrt{3}x(n^2+m^2+nm)^{1/2} I\alpha$. For a current of 10^{-4} A, $\phi/\phi_0 \approx 10^{-4}\alpha$, which is too small to produce significant orbital effects.
[36] M. Hortamani, P. Kratzer, and M. Scheffler, Phys. Rev. B **76**, 235426 (2007).
[37] M. Leadbeater, V. I. Falko, and C. J. Lambert, Phys. Rev. Lett. **81**, 1274 (1998).